Int. J. Multiphase Flow Vol. 13, No. 1, pp. 87–97, 1987
Printed in Great Britain.

0301-9322/87 $3.00 + 0.00

AN IMPROVED MODEL FOR TWO-PHASE FLOW THROUGH BEDS OF COARSE PARTICLES

T. SCHULENBERG† and U. MÜLLER
Institut für Reaktorbauelemente, Kernforschungszentrum Karlsruhe GmbH, Postfach 3640, 7500 Karlsruhe, B.R.D.

(*Received* 4 *April* 1984; *in revised form* 24 *June* 1986)

Abstract—A one-dimensional model for two-phase flow in packed particle beds is presented. Compared with earlier models, the improved model takes into account the effect of interfacial drag forces between liquid and gas, which are of considerable influence in beds of coarse particles. The model is based on the momentum equations for separated flow, which are closed by empirical relations for the wall shear stress and the interfacial drag. The model is applied to the situation of a one-component two-phase flow in an internally heated bed of uniform spherical particles. An increased dryout heat flux is predicted if liquid enters the bed through the bottom.

INTRODUCTION

Two-phase flow through packed beds of coarse particles has become of great interest in the power and process industry. A special application emerged from analysing the hypothetical core meltdown accident of light-water reactors (LWRs). During the course of such an accident fuel rods may be fragmented into particles of irregular shape if the coolant re-enters the damaged core at a very high temperature. Hobbins *et al.* (1982) found that particle size distributions vary strongly with the severity of the rod damage. In particular, coarse particles can be produced if only a thermal and chemical degradation of the rods occurred. The particles are likely to settle on lower and cooler core structures, eventually, at an advanced stage of the accident, even on structures outside the pressure vessel. The particle beds generated in this way are saturated by the coolant. As these particles are still heated by the radioactive decay of the fission products, boiling of the coolant will occur. In order to prevent dryout and finally melting of the debris a two-phase flow model is needed to predict the maximum allowable heat flux through the top of the debris bed.

FUNDAMENTAL EQUATIONS

A laminar two-phase flow model has already been cited by Scheidegger (1974). Following Scheidegger (1974) the pressure drop of a one-dimensional, laminar two-phase flow through a bed of packed particles can be evaluated if the Darcy law is applied to each phase separately. In the case of vertical flow we obtain

$$\frac{\partial p_L}{\partial z} + \rho_L g + \frac{\mu_L}{K K_L} v_L = 0 \qquad [1]$$

and

$$\frac{\partial p_G}{\partial z} + \rho_G g + \frac{\mu_G}{K K_G} v_G = 0. \qquad [2]$$

Here the index L denotes the liquid and the index G denotes the gas phase, v is the superficial velocity, μ and ρ are the viscosity and the density, respectively, g is the acceleration of gravity and p is the pressure. The actual permeability of the bed is composed of the permeability K of a single-phase flow and of the relative permeabilities K_L and K_G, respectively. In the case of uniform

†Present address: Kraftwerk Union AG, Postfach 101153, 4330 Mülheim, B.R.D.

spherical particles the permeability K can be correlated with the particle diameter d and the porosity ϵ:

$$K = \frac{d^2}{150} \frac{\epsilon^3}{(1-\epsilon)^2}. \quad [3]$$

For non-spherical or non-uniform particles K is an empirical constant.

The relative permeabilities K_L and K_G are functions of the effective saturation and of the particle shape. This effective saturation is defined as

$$s = \frac{s^* - s_0}{1 - s_0}, \quad [4]$$

where s^* is the "true saturation", which is the volume fraction of liquid in the space between the particles, and s_0 is the "residual saturation" which remains within the bed if the bed is drained.

The relative permeabilities have been determined by Brooks & Corey (1966) for various sands. For uniform spherical particles their result can be approximated as

$$K_L = s^3 \quad [5]$$

and

$$K_G = (1-s)^3. \quad [6]$$

Because of capillary forces the pressure p_G within the gas phase is generally higher than the pressure p_L in the liquid phase. This pressure difference has been correlated by Leverett (1941) as

$$p_G - p_L = \sigma \sqrt{\frac{\epsilon}{K}} J(s), \quad [7]$$

where σ is the capillary constant and J is a function of the effective saturation and of the particle shape. In most applications J is of the order of $\leqslant 1$. Inserting [7] into [1] and [2] and subtracting [2] from [1], we obtain.

$$\sigma \sqrt{\frac{\epsilon}{K}} \frac{dJ}{ds} \frac{\partial s}{\partial z} + (\rho_L - \rho_G) g + \frac{\mu_L}{K K_L} v_L - \frac{\mu_G}{K K_G} v_G = 0. \quad [8]$$

If $\partial s/\partial z$ is assumed to be of the order of $1/h$, where h is the total bed height, and if dJ/ds is assumed to be of the order of $\leqslant 1$, the capillary pressure term can be neglected against the gravity term if

$$\sigma \sqrt{\frac{\epsilon}{K}} \frac{1}{h} \ll (\rho_L - \rho_G) g. \quad [9]$$

Particles which comply with this restriction are called coarse particles. They are considered here exclusively. As only the product of the particle diameter, which is involved in the permeability, and the bed height enter restriction [9], the model can also be applied to small particles if the bed is sufficiently deep.

The laminar flow model is closed by the balance equations for mass and energy:

$$\epsilon (1 - s_0) \frac{\partial}{\partial t} [\rho_L s + \rho_G (1 - s)] + \frac{\partial}{\partial z} (\rho_L v_L + \rho_G v_G) = 0 \quad [10]$$

and

$$\epsilon (1 - s_0) \frac{\partial}{\partial t} [\rho_G (1 - s)] + \frac{\partial}{\partial z} (\rho_G v_G) = \frac{Q}{h_{LG}}, \quad [11]$$

where Q is the volumetric heat source and h_{LG} is the latent heat of vaporization. These equations are independent of the particle size or shape.

EXTENSION OF THE MODEL

As in single-phase flow, the pressure drop changes continuously from laminar to turbulent flow conditions with increasing particle size. Therefore Lipinski (1982) extended the laminar flow model

by adding a turbulent pressure-drop term to [1] and [2]. An even more realistic model requires an interfacial drag force F_{LG} between liquid and gas to be included in these momentum equations. This has been proposed by Tutu *et al.* (1983). For this case the extended momentum equations read as

$$\frac{\partial p_L}{\partial z} + \rho_L g + \frac{\mu_L}{KK_L} v_L + \frac{\rho_L}{\eta\eta_L} v_L |v_L| - \frac{F_{LG}}{s} = 0 \qquad [12]$$

and

$$\frac{\partial p_G}{\partial z} + \rho_G g + \frac{\mu_G}{KK_G} v_G + \frac{\rho_G}{\eta\eta_G} v_G |v_G| + \frac{F_{LG}}{1-s} = 0. \qquad [13]$$

Here η accounts for the turbulent pressure drop of a single-phase flow through the bed. It has occasionally been termed the "passability" of the bed. For uniform spherical particles this passability has been correlated by Ergun (1952) as

$$\eta = \frac{d}{1.75} \frac{\epsilon^3}{1-\epsilon}. \qquad [14]$$

For particles which are not spherical or which differ in size, η is a further empirical constant. The relative passabilities η_L and η_G are functions of the effective saturation and of the particle shape. Lipinski (1982) assumed that

$$\eta_L = s^3 \qquad [15]$$

and

$$\eta_G = (1-s)^3. \qquad [16]$$

In a recent publication Lipinski (1984) changed the exponents to 5 on the basis of a theoretical work by Reed (1982), but no experimental data are available to validate these theoretical functions. Therefore, in our investigation the functional dependence on the saturation has been determined by measurements, on which we report in the following section.

For modelling the interfacial drag force F_{LG} the following considerations are made.

The force F_{LG} can only be a function of the following four relevant quantities:

—*the buoyant force*

$$(\rho_L - \rho_G) g;$$

—*the viscous forces in the liquid phase with respect to the relative velocities of the phases*

$$\frac{\mu_L}{K}\left(\frac{v_G}{1-s} - \frac{v_L}{s}\right);$$

—*the inertia in the liquid phase with respect to the relative velocity*

$$\frac{\rho_L}{\eta}\left(\frac{v_G}{1-s} - \frac{v_L}{s}\right)^2;$$

—*the capillary force*

$$\frac{\sigma}{K}.$$

In these forces only the relative velocities occur since an interfacial drag is absent if both components have the same velocity. Moreover, the natural length scale for modelling characteristic forces is the particle diameter or, more generally, the permeability and the passability of the bed.

The physical effect creating the viscous force is the shear layer in a separate two-phase flow between the particles. Inertial forces are relevant in dispersed two-phase flow in particle beds, in particular, if the bubbles are of similar size to the interstitial places of the bed. However, no attempt was made to model the microscopic details of the flow.

The buoyant force has also been added to these forces because it is the driving force of the gas in our case of coarse particles. Therefore, [12] and [13] have to be scaled with the buoyant force,

in order to obtain dimensionless equations in which relevant terms are of the same order of magnitude.

Viscous forces and inertia of the gas phase are small compared to the forces discussed above and are therefore neglected. There are strong indications from an experiment by Naik & Dhir (1982) that an interfacial drag force is only relevant in beds of coarse particles. In coarse-particle beds the hydrodynamic interaction is dominated by the turbulent character of the flow; therefore, it is assumed that mainly inertia forces enhance the momentum transfer between both phases. On the other hand, capillary forces will separate the flow and thus reduce the momentum transfer. In the case of bubbly flow, which is expected at high saturation, the viscosity of the liquid may also increase the momentum transfer; however, at lower saturations viscous forces may even stabilize a separated flow and thus reduce the momentum transfer. At moderately high saturations it is expected that the viscosity effects compensate each other. If, for a model of first-order accuracy, only the dominant parameters are taken into account, the interfacial drag force F_{LG}, scaled with the bouyant force, can be modelled such that it depends only on the ratio of inertia/capillary forces and on the effective saturation. The latter effect is expressed by a function $W(s)$ which has to be determined empirically. We obtain

$$\frac{F_{LG}}{(\rho_L - \rho_G)g} = W(s)\frac{\rho_L K}{\eta\sigma}\left(\frac{v_G}{1-s} - \frac{v_L}{s}\right)^2. \qquad [17]$$

In agreement with Tutu *et al.* (1983), F_{LG} is proportional to the square of the relative velocity. However, the dependence on capillary forces is stronger in our model.

EMPIRICAL FUNCTIONS FOR SPHERICAL PARTICLES

The function $W(s)$, which was introduced to describe the interfacial drag force, and the relative passabilities $\eta_L(s)$ and $\eta_G(s)$ are empirical functions which have not been determined yet. Since many experiments in this context have been performed with uniform spherical particles, only these particles have been used during the tests.

Experiments have been performed employing the following test section, shown in figure 1. Almost uniform spherical glass beads of 3 or 7 mm dia were packed into a vertical Plexiglas tube

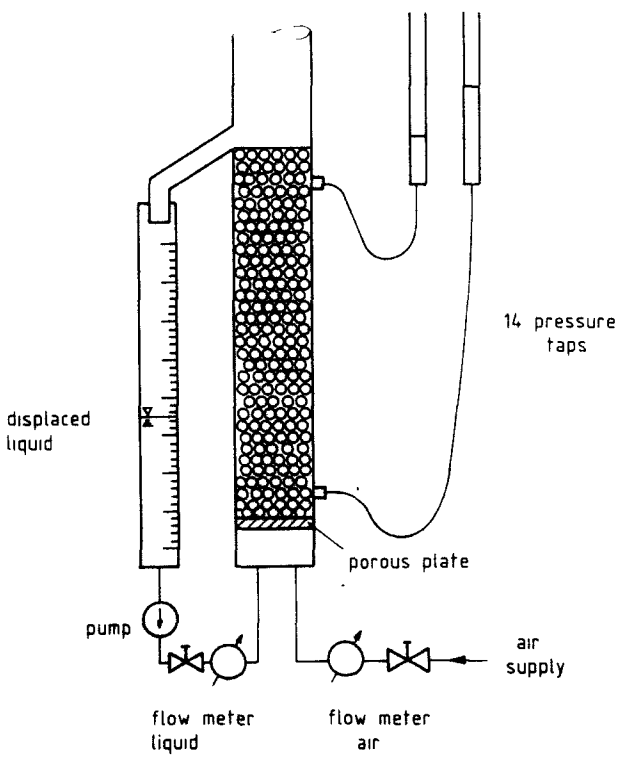

Figure 1. The test section.

Table 1. Properties of the particle beds used in the test section

	Experiment 1	Experiment 2
Mean particle diameter (mm)	3	7
Porosity	0.378	0.412
Permeability (m^2)	5.8×10^{-9}	4.38×10^{-7}
Passability (m)	1.24×10^{-4}	3.87×10^{-3}
Effective particle diameter (mm)	2.5	5.7
Residual saturation in water	0.085	0.024
Residual saturation in 48% ethanol	0.068	—

of 110 mm i.d. and 1 m height. Air and liquid flow rates were measured separately before the two fluids were introduced through a porous plate at the bottom of the bed. The bed was fixed with a grid at the top to prevent fluidization. The pressure drop within the bed was measured with 14 pressure taps of 2 mm dia which were connected with pressure gauges. The saturation was determined from the volume of liquid displaced. Water and an aqueous solution of 48% ethanol were used as test liquids. The tests were run at 20°C and 1 b.

The permeability K and the passability η were determined by pressure-drop measurements of a single-phase flow using water only. The results are listed in table 1. These permeabilities and passabilities are smaller than those obtained from [3] and [14] using the mean particle diameter. Thus, an effective particle diameter can be defined which corresponds to the measured permeability and passability. This effective diameter is smaller than the mean diameter, due to small variations in the particle diameters; only this effective diameter is listed in figures 2–4.

The function $W(s)$ was determined for zero liquid flow rate. Using [12] and [17] with $v_L = 0$, one obtains

$$W(s) = \frac{[\partial p_L/\partial z + \rho_L g](1-s)^2 s}{v_G^2} \frac{\eta\sigma}{\rho_L(\rho_L - \rho_G)gK}. \qquad [18]$$

In figure 2 the experimental results for $W(s)$ are plotted as a function $W(s)/(1-s)$ vs the saturation s. Vertical bars indicate the experimental error bounds. For moderate effective saturations of about 0.6 the same function W was reproduced for different liquids and particle sizes. These facts support the assumptions made in [17]. As the viscosity of 48% ethanol is higher by a factor 2.8 than the viscosity of water, a higher value for $W(s)$ was obtained with ethanol at saturations >0.6. For values <0.5, opposite behaviour can be seen. This result is in accordance with the considerations above concerning the influence of viscosity.

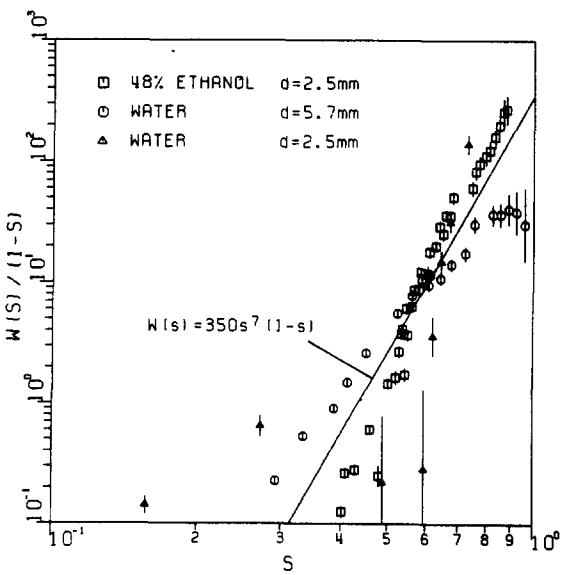

Figure 2. Experimental result for the function $W(s)$.

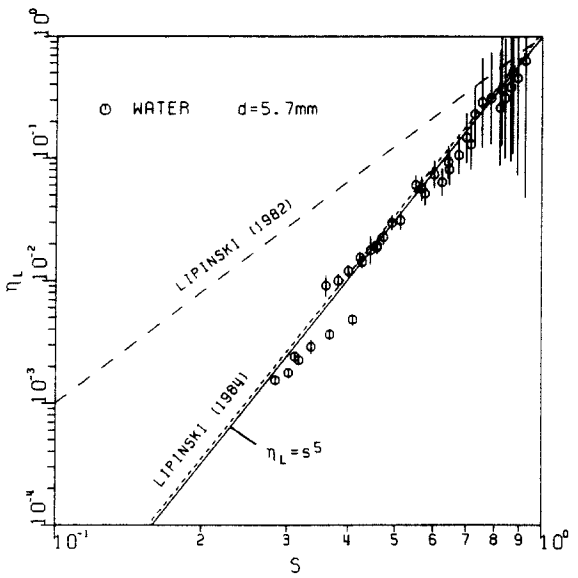

Figure 3. Experimental result for the relative passability η_L of the liquid phase.

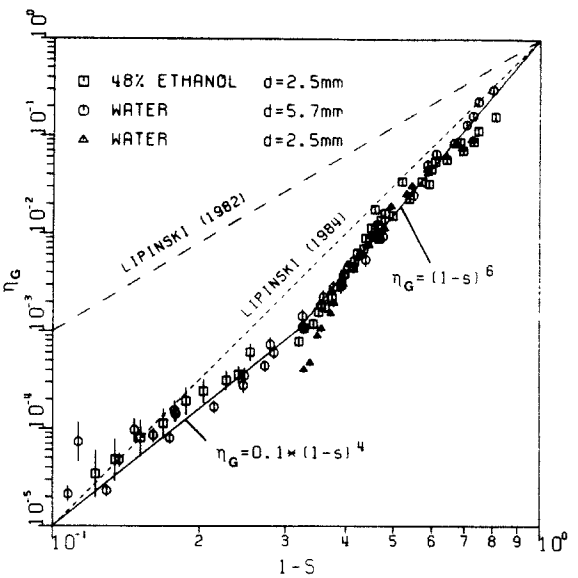

Figure 4. Experimental result for the relative passability η_G of the gas phase.

For all experiments, $W(s)$ can be fitted as

$$W(s) = W_0 s^m (1 - s); \quad [19]$$

$W_0 = 350$ and $m = 7$ can be taken as mean values.

The relative passabilities η_L and η_G have been determined using different liquid flow rates. They can be calculated from [12], [13] and [17], with the relative permeabilities K_L and K_G from [5] and [6], and with the function $W(s)$ from [19]. However, closer approximations for W_0 and m have been used in [19] for individual fluids and particle sizes.

The result for the relative passability η_L of the liquid phase is shown in figure 3. It can be approximated as

$$\eta_L = s^5, \quad [20]$$

which agrees well with the new assumptions of Lipinski (1984).

The result for the relative passability η_G of the gas phase is plotted vs $1 - s$ in figure 4. For saturations below $s = 0.7$ it can be approximated as

$$\eta_G = (1 - s)^6. \quad [21]$$

For saturations above $s = 0.7$ the experimental data slightly exceed this curve. In this range η_G can be better approximated by

$$\eta_G = 0.1 (1 - s)^4. \quad [22]$$

However, for predicting the dryout heat flux of an internally heated debris bed, this latter range of saturations is not relevant. The experimental results for η_G are slightly below the recently assumed correlations of Lipinski (1984).

APPLICATION TO INTERNALLY HEATED DEBRIS BEDS

In the following section our new model, which has been closed by our experimental findings, will be applied to a one-component two-phase flow in internally heated debris beds, such as discussed for certain hypothetical core meltdown accidents of LWRs.

For the calculations the balance equations for mass, [10], and energy, [11], have to be added to the momentum equations [12] and [13]. Only steady-state conditions will be considered. Furthermore, the volumetric heat source Q will be assumed constant. Then [10] and [11] can be integrated

to yield

$$\rho_L v_L + \rho_G v_G = \rho_L v_{L0} + \rho_G v_{G0} \quad [23]$$

and

$$\rho_G v_G = \frac{Qz}{h_{LG}} + \rho_G v_{G0}, \quad [24]$$

where v_{L0} and v_{G0} are the superficial velocities of liquid and vapour, respectively, at $z = 0$ at the bottom of the bed. This bottom is assumed to be adiabatic, so $v_{G0} = 0$, since no vapour enters the bed from below.

The liquid velocity is zero in the case of an impermeable bottom; this is called a top-fed condition because the evaporated liquid can only be replaced through the top of the bed. This case is considered first.

Restricting ourselves to the case of coarse particles, we can neglect the pressure difference between the liquid and vapour. Inserting [23] and [24] into [12] and [13] and subtracting [13] from [12] we obtain the following quadratic equation for the heat flux Qz:

$$\left(\frac{v_L}{v_G}\frac{1}{K_L} + \frac{1}{K_G}\right)\frac{Qzv_G}{Kh_{LG}} + \left\{\frac{\rho_G}{\rho_L}\frac{1}{\eta_L} + \frac{1}{\eta_G} + \frac{W(s)}{s^3(1-s)^3}\frac{\rho_L}{\rho_G} \times \left[s + \frac{\rho_G}{\rho_L}(1-s)\right]^2 \frac{K(\rho_L - \rho_G)g}{\sigma}\right\}\frac{(Qz)^2}{h_{LG}^2 \rho_G \eta} = (\rho_L - \rho_G)g, \quad [25]$$

where v is the kinematic viscosity.

A special solution of [25] is shown in figure 5 for the case of 3 mm spherical particles saturated with water at 1 b. There are two solutions for the heat flux Qz if $Qz < 84\ \mathrm{W/cm^2}$. If the bed was initially filled with liquid only the states of the right branch are realized. Then, for a fixed heat source Q, the right branch shows the vertical distribution of the saturation. If Qz exceeds a maximum, which is called the dryout heat flux, no steady-state solution of Qz exists. In this case

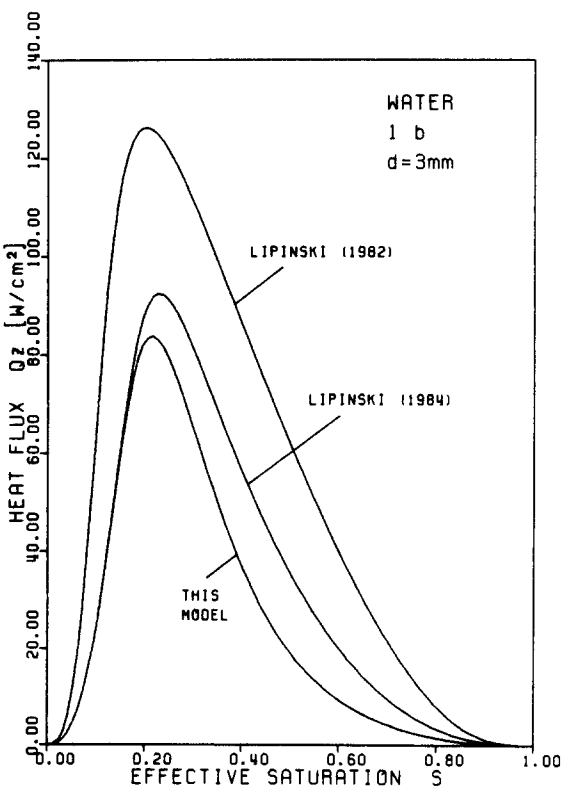

Figure 5. Saturation distribution of an internally heated debris bed under top-fed conditions.

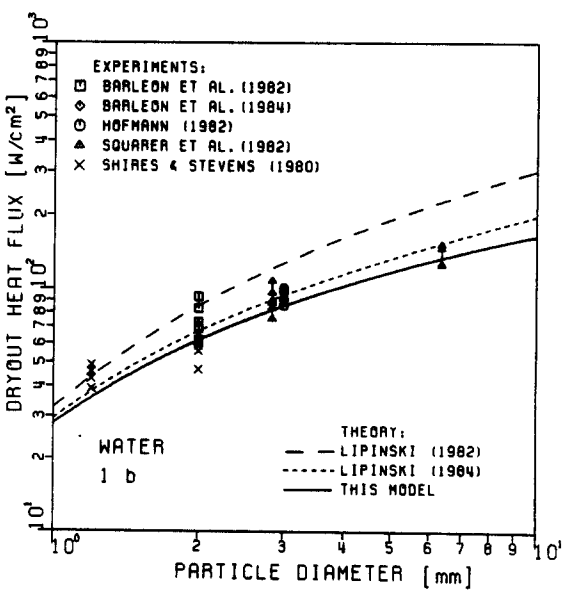

Figure 6. Dryout heat flux of internally heated debris beds under top-fed conditions.

a transient consumption of the liquid reservoir between the two branches will finally lead to a dry region in the bed. This phenomenon was first explained by Hofmann (1982). As the vertical coordinate z cannot exceed the bed height h, the dryout heat flux is equal to the heat flux Qh through the top of the bed under dryout conditions.

This dryout heat flux occurs at saturation <0.3. As we can seen in figure 2 the interfacial drag at these saturations is negligible. Therefore the dryout heat flux of a top-fed bed remains unchanged if interfacial drag forces are included.

In comparison with the predictions by Lipinski (1982, 1984) the dryout heat flux obtained from our model is smaller. This is only due to the different relative passabilities used by Lipinski and ourselves. Moreover, the saturations in the right branch are smaller than those predicted by Lipinski. This effect, however, is also caused by the lack of interfacial drag forces in his model.

Restricting our considerations to beds of uniform spherical particles, we plot in figure 6 the dryout heat flux for water at 1 b vs the particle diameter. For the calculations the porosity was assumed to be $\epsilon = 0.4$. Three predictions are compared with various experiments from the literature. Only those experimental data have been included which comply with restriction [9]. According to figure 5, our predicted dryout heat flux is smaller than the values proposed by Lipinski (1982, 1984).

Compared with the experimental results our model agrees well with a lower bound of the dryout heat flux found in experiments. This agreement seems to be reasonable considering that an increased dryout heat flux in the experiments can be explained by a residual amount of capillary forces, which have been neglected in our model, and by a loosening of the particles in the upper part of the bed which is caused by the rising vapour. The latter effect is also not accounted for in our model.

Information about the influence of interfacial drag forces can be obtained, if debris beds are considered which are arranged on permeable support structures. In this case v_{L0} is different from zero. The arrangement is called a bottom-fed condition. The same procedure as for top-fed conditions, but with $v_{L0} = 0$, yields the following quadratic equation for the heat flux Qz:

$$\left(\frac{v_L}{v_G}\frac{1}{K_L}+\frac{1}{K_G}\right)\frac{Qzv_G}{Kh_{LG}}-\frac{\mu_L v_{L0}}{KK_L}+\frac{1}{\eta\eta_G}\frac{(Qz)^2}{\rho_G h_{LG}^2}-\frac{1}{\eta\eta_G}\rho_L v_L|v_L| + W\frac{K(\rho_L-\rho_G)g\rho_L}{\sigma\eta}\frac{1}{s(1-s)}\left[\frac{1}{(1-s)}\frac{Q_z}{\rho_G h_{LG}}-\frac{v_L}{s}\right]^2=(\rho_L-\rho_G)g,$$

with

$$v_L = -\frac{Qz}{\rho_G h_{LG}} + v_{L0}. \qquad [26]$$

The solution of this equation can be inserted into [12] so that the pressure gradient can be determined at each elevation. After integration we obtain the vertical pressure distribution within the bed. This pressure distribution is shown in figure 7 for uniform spherical particles of 4.763 mm dia, saturated with Freon-113 at 1 b. The pressure has been scaled with the hydrostatic pressure of the liquid. The heat flux through the top of the bed can be obtained from the exit quality x_e, indicated in figure 7, as

$$Qh = \rho_G h_{LG} v_{L0} x_e.$$

Comparison with results based on the model of Lipinski (1984) shows that the effect of interfacial drag forces is to reduce the pressure of the two-phase mixture remarkably below the hydrostatic pressure of the liquid. This effect is supported by the experimental results of Tung *et al.* (1983). Predictions based on a homogeneous model of Naik & Dhir (1982) overestimate the interfacial drag.

Further support for the validity of our model is provided by an experiment of Naik & Dhir (1982). In figure 8 the total pressure drop across a bed of 4.763 mm spheres, saturated with water at 1 b, is plotted vs the fluid velocity v_{L0} at the bottom of the bed. Data are shown for various exit qualities x_e at the bed surface. In agreement with our model the experimental pressure drop falls more than 30% below the hydrostatic pressure of the liquid, which is in clear contradiction with predictions if the model of Lipinski (1984) is applied, which neglects the interfacial drag.

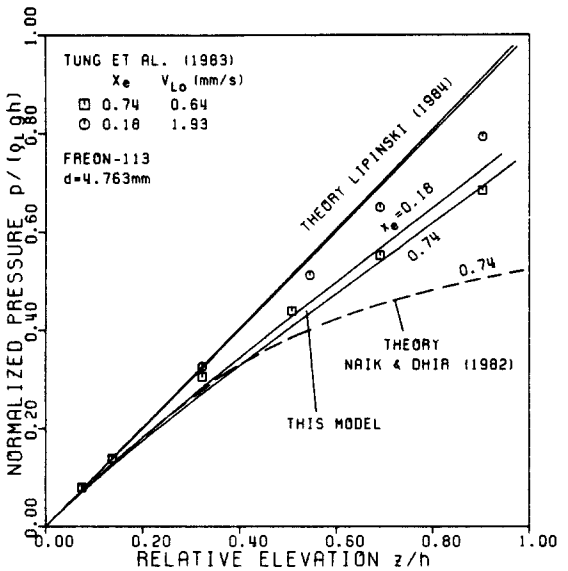

Figure 7. Vertical pressure distribution in an internally heated debris bed under bottom-fed conditions.

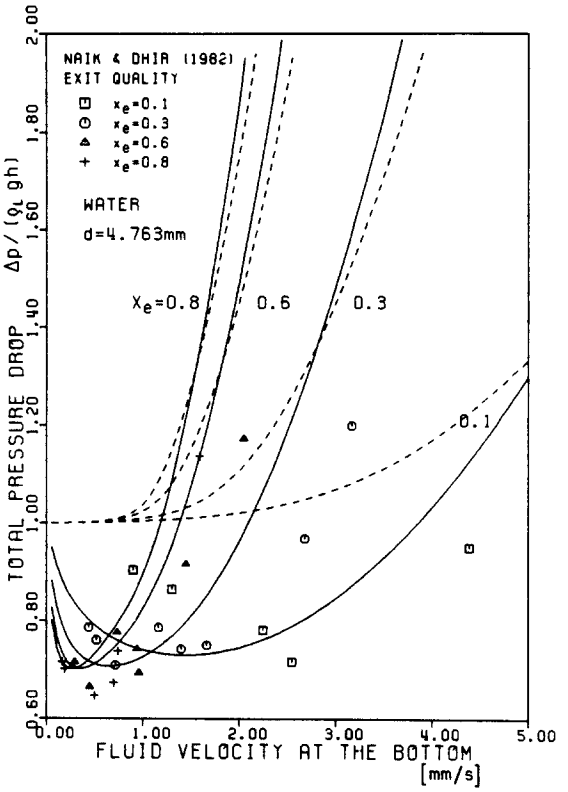

Figure 8. Total pressure drop across a bottom-fed debris bed. ——, this model; – – –, theory of Lipinski (1984).

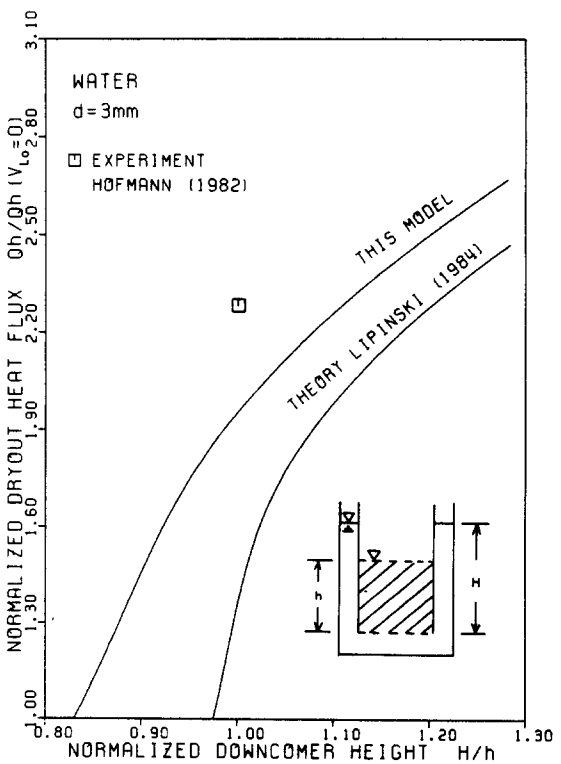

Figure 9. Dryout heat flux of an internally heated debris bed with a downcomer-driven bottom injection.

This reduction in the total pressure drop could significantly enhance the coolability of a debris bed in the case of core meltdown accidents in LWRs. It has been demonstrated by Hofmann (1982) and Stevens & Trenberth (1982) that a permeable support structure beneath the bed increases the dryout heat flux, if the flow entering at the bottom is driven by the hydrostatic pressure of the liquid in a downcomer surrounding the bed.

In figure 9 the dryout heat flux of a bottom-fed debris bed of 3 mm spheres, saturated with water at 1 b, is given as a function of the water level in the surrounding annulus, subsequently called downcomer. The dryout heat flux has been scaled with the dryout heat flux of a top-fed bed on an impermeable adiabatic plate, and the downcomer height has been scaled with the height of the bed. Our model is supported by an experiment of Hofmann (1982), which is also plotted in figure 9. In the absence of interfacial drag forces, as assumed by the model of Lipinski (1984), the increase in the dryout heat flux is underestimated if the normalized downcomer height is of the order of $\leqslant 1$.

SUMMARY AND CONCLUSION

A one-dimensional model for two-phase flow through beds of packed particles has been developed. Compared with earlier models it includes in addition the influence of interfacial drag forces between liquid and gas. These forces are expressed by a simple relation containing the dominant ratio of liquid inertia/capillary forces. The influence of liquid viscosity is found to be of less importance and is therefore neglected. In an initial stage the model is restricted to coarse particles or deep beds so that the pressure difference between both phases is negligible. In this case the saturation distribution can be determined algebraically.

The model can be applied to particles of any shape provided that the empirical functions, which the model needs, are available. These functions depend only on the effective saturation. They are, in general:

—the relative permeabilities $K_L(s)$ and $K_G(s)$, which are important in beds of fine particles and in the case of slow velocities;
—the relative permeabilities $\eta_L(s)$ and $\eta_G(s)$, which are important in beds of coarse particles and in the case of high velocities;
—the Leverett function $J(s)$, which is important in shallow beds of fine particles;
—the interfacial drag function $W(s)$, which is important in beds of coarse particles, especially in the case of high saturation.

For the special case of uniform spherical particles these functions have been determined experimentally.

Although these functions were obtained using water and air and an aqueous solution of 48% ethanol and air, they agree well with earlier experimental results obtained with water and vapour and with Freon-113 and Freon vapour at 1 b. This agreement confirms the validity of our model for arbitrary fluids.

The coolability of an internally heated debris bed has been discussed, which is expected after a core melt down accident in an LWR. If this bed is arranged on an impermeable, adiabatic support structure, the dryout heat flux is predicted to be a little smaller than, but similar to, recent predictions by Lipinski (1984). The interfacial drag has no influence on this dryout heat flux. However, if additional fluid can be supplied through the bottom of the bed, interfacial drag forces may significantly increase the downcomer-driven bottom-inlet mass flux, and hence the coolability of the bed. In this case our model is in a better agreement with experimental results than the model of Lipinski (1984), which does not include an interfacial drag.

Acknowledgements—The authors wish to thank T. Kastner for preparing the test section and E. Wiens for performing numerous measurements.

REFERENCES

BARLEON, L., THOMAUSKE, K. & WERLE, H. 1982 Dependence of dryout heat flux on particle diameter and effects of stratification and bed reconfiguration. In *Post Accident Debris Cooling* (Edited by MÜLLER, U. & GÜNTHER, C.), pp. 74–78. Braun, Karlsruhe.

BARLEON, L., THOMAUSKE, K. & WERLE, H. 1984 Cooling of debris beds. *Nucl. Technol.* **65,** 67–86.

BROOKS, R. H. & COREY, A. T. 1966 Properties of porous media affecting fluid flow. *J. Irrig. Drain. Div. Am. Soc. civ. Engrs* IR2, **92,** 61–89.

ERGUN, S. 1952 Fluid flow through packed columns. *Chem. Engng Prog.* **48,** 89–94.

HOBBINS, R. R., COOK, B. A. & MASON, R. E. (1982) LWR debris from severe in-pile transient tests. In *Post Accident Debris Cooling* (Edited by MÜLLER, U. & GÜNTHER, C.), pp. 133–138. Braun, Karlsruhe.

HOFMANN, G. 1982 On the location and mechanism of dryout in top-fed and bottom-fed particulated beds. In *Post Accident Debris Cooling* (Edited by MÜLLER, U. & GÜNTHER, C.), pp. 186–191. Braun, Karlsruhe.

LEVERETT, M. C. 1941 Capillary behaviour in porous solids. *Trans. Am. Inst. Min. Engrs* **142,** 152–168.

LIPINSKI, R. J. 1982 A model for boiling and dryout in particle beds. Reports NUREG/CR-2646, SAND 82-0765.

LIPINSKI, R. J. 1984 A coolability model for post-accident nuclear reactor debris. *Nucl. Technol.* **65,** 53–66.

NAIK, A. S. & DHIR, V. K. 1982 Forced flow evaporative cooling of a volumetrically heated porous layer. *Int. J. Heat Mass Transfer* **25,** 541–552.

REED, A. W. 1982 The effect of channeling on the dryout of heated particulate beds immersed in a liquid pool. Ph.D. Thesis, MIT, Cambridge, Mass.

SCHEIDEGGER, A. E. 1974 *The Physics of Flow Through Porous Media.* Univ. of Toronto Press, Toronto.

SHIRES, G. L. & STEVENS, G. F. 1980 Dryout during boiling in heated particle beds. Report AEEW-M 1779, UKAEA, Winfrith, Dorset.

SQUARER, D., PIECZYNSKI, A. T. & HOCHREITER, L. E. 1982 Effect of debris bed pressure, particle size, and distribution on degraded nuclear reactor core coolability. *Nucl. Sci. Engng* **80,** 2–13.

STEVENS, G. F. & TRENBERTH, R. 1982 Experimental study of boiling heat transfer and dryout in heat generating particulate beds in water at 1 bar. In *Post Accident Debris Cooling* (Edited by MÜLLER, U. & GÜNTHER, C.), pp. 108–113. Braun, Karlsruhe.

TUNG, V. X., DHIR, V. K. & SQUARER, D. 1983 Forced flow cooling studies of volumetrically heated porous layers. In *Thermal Hydraulics of Nuclear Reactors* (Edited by MERILO, M.), pp. 876–883. ANS, La Grange Park, Ill.

TUTU, N. K., GINSBERG, T. & CHEN, J. C. 1983 Interfacial drag for two-phase flow through high permeability porous beds. In *Interfacial Transport Phenomena* (Edited by CHEN, J. C. & BANKOFF, S. G.), pp. 37–44. ASME, New York.